Astronomical and Astrophysical Transactions (*AApTr*), 2025, Vol. 35, Issue 3, pp. 291–300,
ISSN 1055-6796, Photocopying permitted by license only, ©Cambridge Scientific Publishers

First detailed study of the eccentric binary 2MASS 22425392+5439498 using multi-survey data

F.B. Khamrakulov[1,*], O.A. Burkhonov[2], E.G. Lapukhin[3], S.Sh. Ergashev[1]

[1] *Department of Nuclear Physics and Astronomy, Samarkand State University, Samarkand 140104, Uzbekistan*
[2] *Ulugh Beg Astronomical Institute, Uzbekistan Academy of Sciences, Astronomicheskaya 33, Tashkent 100052, Uzbekistan*
[3] *Reshetnev Siberian State University of Science and Technology, Krasnoyarsky Rabochy Av. 31, Krasnoyarsk 660014, Russia*

Received 27 April, 2025; accepted 29 May, 2025

We present the first comprehensive photometric and orbital analysis of the detached eclipsing binary 2MASS 22425392+5439498, utilizing multi-survey data from Lapukhin, ASAS-SN, and TESS. The study combines light curves spanning over a decade to determine the orbital period, eccentricity, and evidence for apsidal motion in this previously uncharacterized system. When modeling this system based on photometric data using the JKTEBOP program, we accounted for third-light contamination from a line-of-sight star, limb darkening, and the system's orbital geometry parameters. The secondary minimum occurs at phase $\phi = 0.4940$, indicating a small but significant eccentricity. Based on the modeling results, we estimate the apsidal motion of the system to be very slow (i.e., the apsidal period is very large), and therefore, this motion does not significantly affect the depth of the eclipses.

Keywords: Data surveys, binaries: eclipsing, orbital and apsidal parameters, modeling

1 Introduction

Mutual eclipses of the components can occur in the system if the orbit's inclination is not much different from 90°. Systems Algol (Persei), Lyra, and W Ursae Majoris comprise the three classifications of classical eclipsing binaries according to the shape of the corresponding light curve. Eclipses and nearly continuous out-of-eclipse brightness zones cause primary and secondary minima in Algol-type systems (Cherepashchuk, 2022). Binary star systems with elliptical orbits exhibit a fundamental dynamical phenomenon known as apsidal motion, or the secular advance of periastron. For many years, these ideas of stellar system have been tested by analyzing apsidal motion in eccentric binary stars. The finite size of the stellar components

*Email: x-farxodjon@mail.ru

and the tidal interactions between them directly result in the periastron progress of an eccentric binary system (Sterne, 1939).

Understanding apsidal motion in eclipsing binaries is essential for understanding interior distributions of matter, star structure (Kozyreva et al., 2024), and the viability of gravitational theories outside of our solar system (Claret Giménez , 2010). Detachable, eccentric eclipsing binaries are very helpful for evaluating general relativity because the relativistic influence becomes substantial in systems with higher total masses and shorter orbital periods (Wolf et al , 2010).

Eclipsing binary 2MASS 22425392+5439498 was identified as a detached eclipsing binary system of the EA type, with an average orbital period of 2.24636 days by (Lapukhin et al , 2020) based on observations at the SIBSAU observatory along with more than 100 other new variable stars. Since this object is bright, its observations appear in many catalogs under different designations: V0926 Lac, TIC 388963111, ASASSN-V J224253.95+543949.7.

2 Observation and data reduction

This star was included as V0926 Lac to the General Catalogue of Variable Stars (GCVS) (Samus' et al., 2017), (Kazarovets et al., 2023). The object's coordinates are $\mathrm{RA_{J2000.0}} = 22^{\mathrm{h}}42^{\mathrm{m}}53.954^{\mathrm{s}}$, $\mathrm{Dec_{J2000.0}} = +54^{\circ}39'50.167''$, with a distance of 1227.45 ± 32.3924 pc (Gaia Collaboration , 2020). The effective temperature (T_{eff}) of 7076 ± 135.126 K, stellar radius of 2.08795 ± 0.0924121 $R_{\odot}$, stellar mass of 1.57 ± 0.269087 $M_{\odot}$, and distance of 1247.39 ± 25.655 pc, as determined from the TESS Input Catalogue, were compared with results from other catalogues (Stassun et al , 2019). The source identified in the Gaia catalogue as DR3 2003232640188743680 has an effective temperature (T_{eff}) of $=7439 \pm 336$ K (Bai et al , 2019). Based on this comparison, a reliable conclusion was drawn.

To analyze the apsidal motion and determine orbital parameters of the object 2MASS22425392+5439498, we utilized observational data obtained at different times from Lapukhin, ASASSN-V, and TESS.

The ZTF project (Bellm et al , 2019) obtained observations of 2MASS 22425392+ 5439498 between 2015 and 2018. However, the resulting light curves are fragmented into separate segments with gaps of approximately one day. Due to this discontinuity, the ZTF data are not well suited for determining precise times of minima from individual light curves. Consequently, we do not incorporate these data in the present analysis.

2.1 Observation data by Lapukhin

The photometric measurement results obtained by Lapukhin et al (2020) were taken from the Peremennye Zvezdy Prilozhenie. The initial observations were conducted by Lapukhin at the Reshetnev Siberian State University of Science and Technology Observatory using the Hamilton Telescope ($D = 400$ mm, $F = 915$ mm) during the periods of August–October 2012 and September–October 2014. The field of view (FoV) is 2.3×2.3 degrees. The telescope was equipped with an FLI ML9000 CCD chip (3056×3056 pixels, pixel size 12 μm). All CCD observations were conducted

without a filter, with an exposure time of 30 seconds for all frames. The exposure time was determined empirically, with a limiting magnitude of approximately 16–17^{m} (Lapukhin et al , 2020). The observational uncertainty for 2MASS 22425392+5439498 is $\sigma = 0.01176$. Due to the presence of a bright star near the primary object, smaller values were chosen for the object aperture, inner annulus, and outer annulus during aperture photometry in order to minimize contamination in the observational results. The analysis of the observational results obtained by Lapukhin was performed using the VaST software (Sokolovsky and Lebedev , 2018).

2.2 ASAS-SN observation data

The All-Sky Automated Survey for Supernovae (ASAS-SN) is a wide-field optical survey designed to monitor the entire sky for transient and variable phenomena. The survey utilizes a network of small-aperture Nikon telephoto lenses 14 cm telescopes equipped with CCD cameras, providing long-term photometric coverage with high cadence. The field of view of a single ASAS-SN camera is 4.5 deg^2, the pixel scale is 8.0 arcsec, and the full width at half-maximum (FWHM) is ∼2 pixels. The ASAS-SN cameras capture three 90 s images for every epoch, which are merged to improve the signal-to-noise ratio (SNR) (Jayasinghe et al , 2018). The ASAS-SN Variable Star Catalog (ASASSN-V) catalogs periodic and non-periodic variables using ASAS-SN observations and classifications based on Gaia, 2MASS, and AllWISE data. The publicly available database provides light curves for detailed studies of stellar variability (Christy et al , 2023). In this study, 2MASS 22425392+5439498 (ASASSN-V J224253.95+543949.7) ASASSN-V[1] photometric data was used to refine the periods, classifications, apsidal motion, and orbital parameters of selected stars.

2.3 TESS observation data

The space observatory TESS (Transiting Exoplanet Survey Satellite) uses four identical cameras to observe stars over a total 24° × 96° field of view to observe pre-defined sectors. Each sector lasts 27 days and is nearly continuous, with a brief midpoint pause for momentum unloading and data transmission (Ricker et al , 2015). The TESS mission observed 2MASS 22425392+5439498 (in the TESS identified name is TIC 388963111) in sectors 16 (2019/09/12 to 2021/02/20), 17 (2019/10/08 to 2020/12/04), 57 (2022/09/30 to 2023/06/27), 77 (2024/03/25 to 2024/08/16) and 84 (2024/10/01 to 2025/02/21). The reduced data were downloaded from the MAST[2] archive and converted from flux units to relative magnitude. Since the analysis results were similar, the data from sector 16 were selected. Each photometric point is assigned a QUALITY flag which indicates if the data has been compromised to some degree by instrumental effects. We removed those points which did not have QUALITY = 0 and normalized each light curve by dividing the flux of each point by the mean flux of the star. 2MASS 22425392+5439498 has a two neighbor stars a) (22:42:54.2121310 +54:39:56.202791) and b) (22:42:54.4090487 +54:39:50.678584) that affects its brightness due to the presence of third light (Figure 1). The contamination value for the star TIC 388963111 is 0.4903898, which is larger than the light

[1]https://asas-sn.osu.edu/photometry
[2]https://mast.stsci.edu/portal/Mashup/Clients/Mast/Portal.html

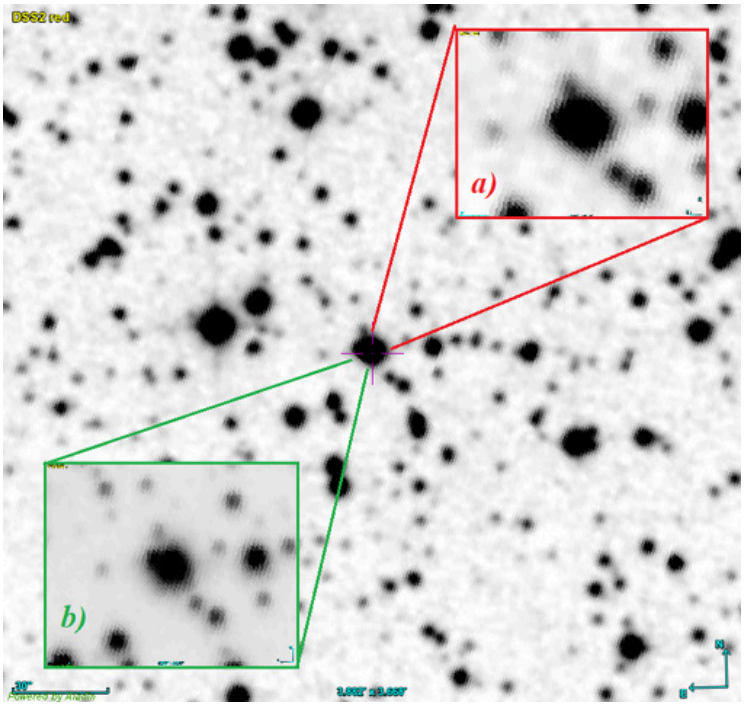


Figure 1 The map of 2MASS 22425392+5439498 region. At the center of the field is shown in the DSS2 Red (F+R) image. The zoomed-in view of the neighboring stars is presented in: (a) DSS2 Red (F+R) and (b) ZTF DR7 r-band images.

contamination coefficient value of 0.36 reported by the TESS Asteroseismic Science Operations Center (TASOC) (Handberg et al , 2021). Therefore, the contamination value calculated for the star TIC 388963111 of 0.4903898 does cause a very small partial effect on its photometric results. The presence of a nearby neighboring stars in the frame (Figure 1) could potentially explain only half of the third light found from the analysis of the all light curves. Since the object's brightness is sufficiently high, the influence of both neighboring stars on its brightness was taken into account in the analysis.

3 Light curves analysis

For each photometric data of the object V0926 Lac (Lapukhin, ASASSN-V, and TESS), the accurate period was identified using the online Period Search Service[3], which turned out to be equal to 2.2455913 days. Based on the accurately determined period, phase light curves were constructed for each photometric data. The green data points representing Lapukhin's observations reveal a slight displacement of the secondary minimum from phase $\phi = 0.5$, as evident from a visual inspection of the

[3]https://scan.sai.msu.ru/lk/

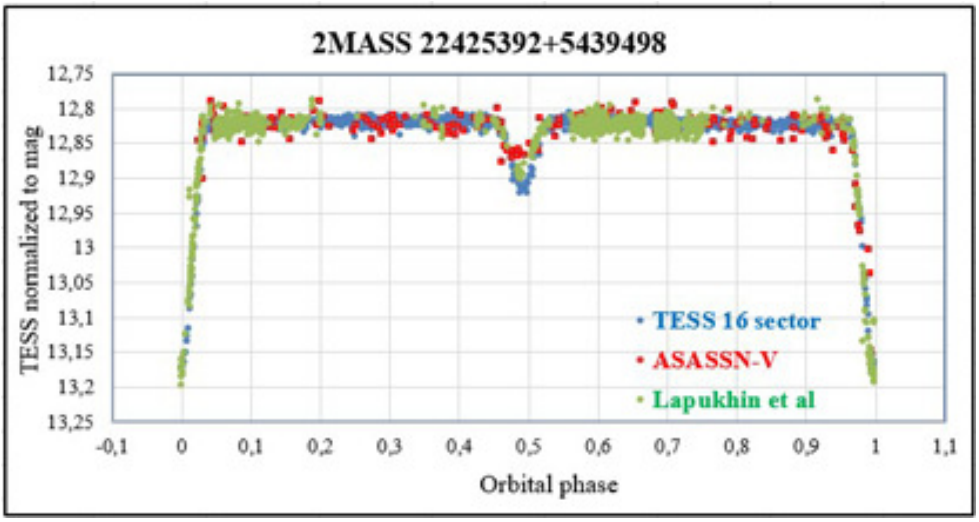


Figure 2 The phase light curve, combining the observation results from Lapukhin, ASASSN-V, and TESS, is presented as an overlaid plot in a graph.

light curve. This displacement becomes more pronounced when zooming in on the corresponding section of the phase plot (Figure 2 for comparison). The secondary minimum is observed at phase $\phi = 0.4940$, indicating a slightly elliptical orbit. The phase brightness curves of 2MASS 22425392+5439498 in Figure 2 exhibit different magnitude values due to the use of different filters in the ASASSN-V (V band) and TESS (bandpass) (Ricker et al , 2015) observations, as well as the unfiltered observations conducted by Lapukhin.

To correct for these discrepancies and standardize the magnitudes in Fig. 2, a correction of –0.34575 was applied to Lapukhin's photometric measurements, while a correction of –0.30826 was added to the ASASSN-V photometric data. The TESS photometric measurements were used as the reference for normalization. The phase of the secondary minimum (Min II) with respect to the phase of primary minimum (Min I) is 0.4940. Along the vertical axis, we show the brightness of the star normalized to that outside minimum.

3.1 Modeling binary system

Version 43 of the JKTEBOP[4] was used to model the light curves from each of the three photometric data. We fitted for the sum and ratio of the fractional radii of the stars, expressed as their sum $r_A + r_B$ and ratio $k = r_B + r_A$ the orbital inclination i, the central surface brightness ratio J, the amount of contaminating light $L3$ and the coefficients of the reflection effect. The orbital eccentricity e and argument of periastron ω were included using the elements $e\cos\omega$ and $e\sin\omega$. The secondary eclipse was found to occur at orbital phase 0.4940. Limb darkening was represented

[4]https://www.astro.keele.ac.uk/jkt/codes/jktebop.html

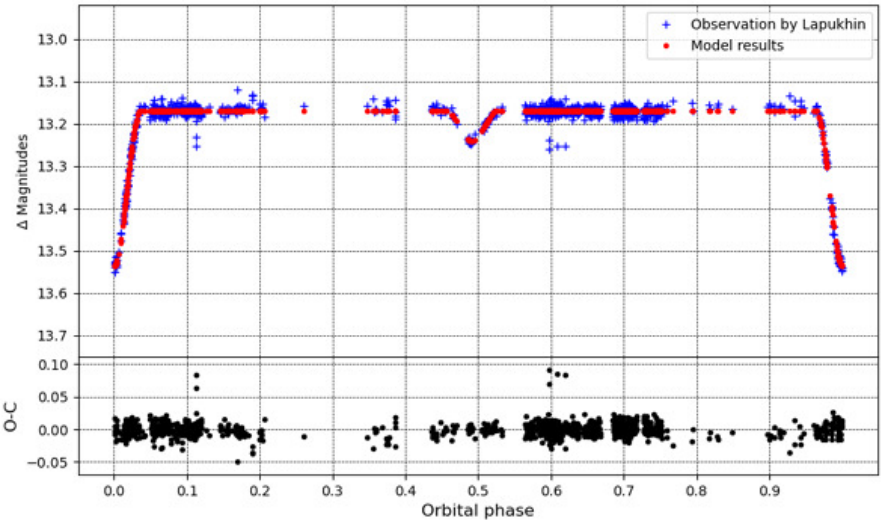


Figure 3 The light curve and the corresponding model based on photometric results obtained from observations of the object 2MASS 22425392+5439498 by Lapukhin. The lower panels display the residuals of the fit, with the zero-residual line overlaid in white for clarity.

using the quadratic law, the coefficients were assumed to be the same for both stars, the linear coefficient was fitted, and the nonlinear coefficient was fixed to a suitable value from (Claret , 2018, 2000). These assumptions were checked and found to have a negligible impact on the best fits. Lapukhin, ASASSN-V and TESS (16 sector) data were analyzed separately using JKTEBOP for each result. The primary and secondary eclipses have significantly different depths. The amount of third light L_3 has a significant effect on the best-fitting parameter values.

If fitted, it converges to a formally significant but unphysically negative value (–1.4845 ± 1.556) despite the negligible amount of light from nearby stars. We therefore fixed it at zero in our default solution, but added contributions to the error bars based on the change in parameter values by assuming $L_3 = 17\%$ instead. For information, such an assumption decreases r_A by 5.2% and increases r_B by 3.2%. Due to the limited number of observations conducted by Lapukhin and the presence of observational errors, discontinuities and scatter can be observed in the flat regions of the light curve. Based on the analyzed photometry results the light curve was modeled and the best-fit model was constructed. As a result, the parameters presented in Table 1 column 1 were accurately determined.

Finally, we applied polynomial fits to the overall brightness of the system to deal with any slow changes in brightness, likely of instrumental origin, during the TESS observations. The best JKTEBOP fit to the TESS data is shown in Fig. 4. The residuals have a hint of a non-Gaussian distribution to them – they scatter more to fainter than brighter magnitudes – an effect that we have often seen in TESS light curves. The parameters of the fit are given in Table 1 column 2. The secondary eclipse occurs at orbital phase 0.4940.

Table 1 Parameters of the best JKTEBOP fit to Lapukhin, TESS and ASASSN-V light curve of 2MASS 22425392+5439498.

Parameter	2MASS 22425392+5439498	TIC 388963111	ASASSN-V J224253.95+543949.7
Time of primary eclipse (HJD-2450000)	$6928.0820951 \pm 0.0001172$	$8740.9221807 \pm 0.0009596$	$7938.9576554 \pm 0.0005165$
Orbital period (day)	2.2463655 ± 0.0000016	2.2463199 ± 0.0001585	2.2463868 ± 0.0000019
Orbital inclination (°)	81.8679 ± 1.3904	84.7972 ± 2.1380	81.7948 ± 0.1865
Sum of the fractional radii	0.2270 ± 0.0086	0.2644 ± 0.0302	0.3842 ± 0.0033
Ratio of the radii	0.500010 ± 0.000021	0.500001 ± 0.000013	0.500000 ± 0.000019
$e \cos \omega$	-0.01329 ± 0.00071	-0.01226 ± 0.00153	-0.00827 ± 0.00065
$e \sin \omega$	-0.07501 ± 0.02740	-0.13858 ± 0.11181	0.63423 ± 0.02922
Central surface brightness ratio	0.0766 ± 0.0726	0.0736 ± 0.1117	0.3341 ± 24.3370
Third light (L)	-0.3159 ± 0.3005	-1.4845 ± 1.5566	-1.5458 ± 3.6115
LD (A) coefficient c	0.9351 ± 0.1254	1.1567 ± 0.6637	0.3597 ± 0.2356
LD (B) coefficient α	11.1386 ± 6.3324	12.2223 ± 0.7248	18.2020 ± 7.3425
Derived parameters			
Fractional radius of star A	0.15132 ± 0.00007	0.17629 ± 0.00005	0.25612 ± 0.00001
Fractional radius of star B	0.07566 ± 0.00004	0.08815 ± 0.00005	0.12806 ± 0.000005
Eccentricity	0.13618 ± 0.00013	0.13912 ± 0.00025	0.13429 ± 0.00062
Argument of periastron (°)	263.1520 ± 0.021	264.1445 ± 0.047	263.7468 ± 0.011
Light ratio ℓ_B/ℓ_A	0.05316 ± 0.0038	0.05646 ± 0.0043	0.05255 ± 0.0016

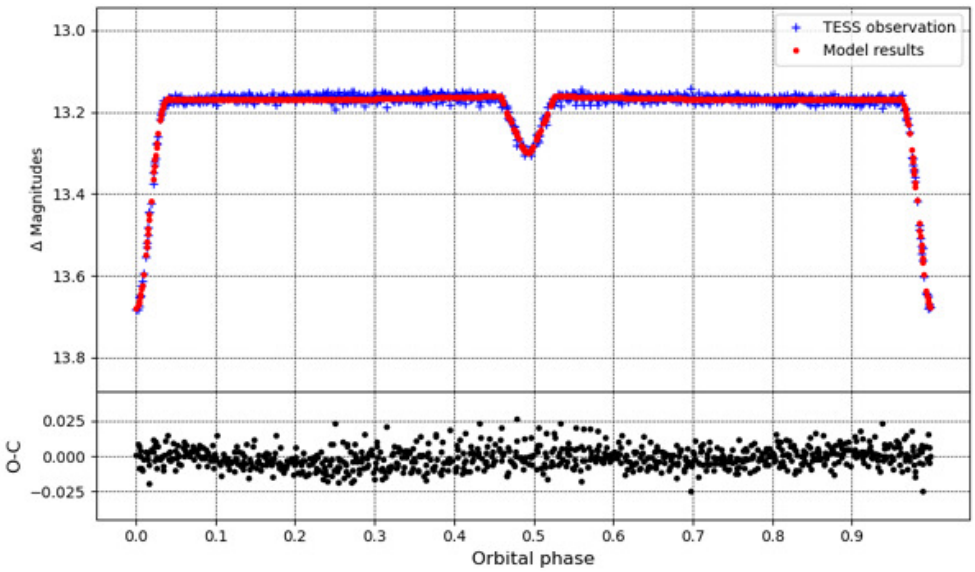


Figure 4 Best fitting model results to the TESS sector 16 light curve of TIC 388963111. The residuals are shown on an enlarged scale in the lower panel.

4 Discussion

Fundamental stellar systems that supply both the orbital (such as period, eccentricity, and longitude of periastron) and physical (such as radius, temperature, and luminosity) parameters are eclipsing binaries, particularly those with eccentric orbits. These two parameters set enable the computation of the synchronization and circularization timescales as well as the testing of various tidal hypotheses. The EA-type

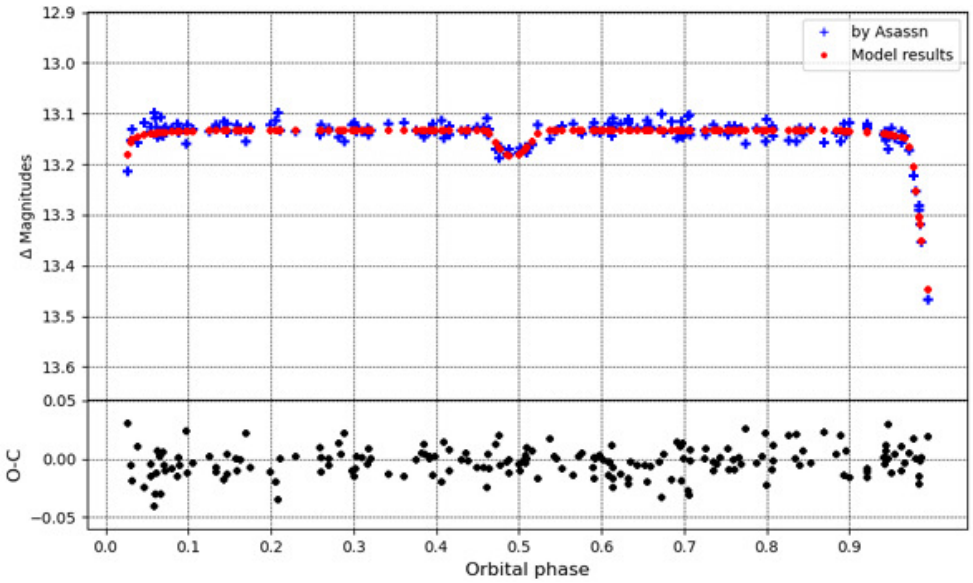


Figure 5 The light curve and the corresponding model based on photometric results of the object ASASSN-V J224253.95+543949.7 obtained by ASASSN. The two highest and two lowest residual values in the light curve (below).

object 2MASS 22425392+5439498, discovered by Lapukhin et al., was reanalyzed using aperture photometry data from the TESS and ASASSN-V databases, along with Lapukhin's original photometric results. The analysis revealed that the system possesses an eccentric orbit. Based on theoretical calculations, a model consistent with the photometric data was constructed using the JKTEBOP program. This model was then used to derive orbital parameters (Table 1). The determined values of e and ω should be regarded as preliminary since we only know photometric light curves and inadequately trustworthy properties of both components in binaries, such as effective temperatures, mass ratio, etc. Additionally, light fluctuations outside eclipses may affect light curve modeling results, which low-order polynomials cannot eliminate. The phase light curves of the eclipsing binary are shown in Figures 3, 4, and 5. The solid curve is the model that was computed using the JKTEBOP, and the dots represent the observational data. The variations in orbital inclination and argument of periastron presented in Table 1 are related to the observation times at different epochs. The significant discrepancies in the remaining parameters may be attributed to the limited and potentially inaccurate observational data from ASASSN-V and Lapukhin, as well as the possible influence of third light. The TESS photometric results were evaluated as the best-fitting and most accurate model.

5 Conclusion

Our analysis reliably confirms that the object 2MASS J22425392+5439498 is an eclipsing binary system, validating the preliminary conclusions made by its discoverers. Due

to the high quality, large volume, and low measurement errors of the TESS photometric data, the model constructed based on these observations was considered the most reliable. Accordingly, this model was applied to the photometric data obtained by Lapukhin and from the ASAS-SN survey. Despite the limited number of data points in these two datasets, we were able to successfully construct corresponding models, the results of which closely match those derived from the TESS observations. The orbital period we determined 2.2455913 days is consistent with the model values derived from all the datasets used, within the margin of error. The difference between the orbital inclination derived from the TESS data $84.797 \pm 2.14^{\circ}$ and that derived from the Lapukhin and ASAS-SN data is most likely attributable to differences in photometric data density and the epochs of observations. Similarly, discrepancies in other model parameters, such as eccentricity, are likely due to the same factors.

Our analysis also indicates that the eclipse depths do not vary in antiphase, and the estimated apsidal motion period of the system is excessively long. Therefore, we conclude that apsidal motion is unlikely to have a significant effect on the eclipse depth.

Acknowledgments

We express our gratitude to our colleagues from the Galactic Astronomy laboratory of the Astronomical Institute and the Department of Nuclear Physics and Astronomy, Samarkand State University, for their participation in the discussion of the obtained results.

References

Cherepashchuk A.M 2022. Astronomy Reports 66. S5-S69

Sterne TE. 1939. Apsidal motion in binary stars. Monthly Notices of the Royal Astronomical Society 99: 451-62.

Kozyreva VS, Khamrakulov F.B, Burkhonov OA, Bogomazov AI, Satovskiy BÂL. 2024. Rotation of the Apsidal Line in the Eclipsing System V1059 Cep. Astronomy Reports 68: 48-5

Claret A, Giménez A. 2010. The apsidal-motion test of stellar structure and evolution: an update. Astronomy and Astrophysics 519: A57

Wolf M, Claret A, Kotková L, Kučáková H, Kocián R, et al. 2010. Relativistic apsidal motion in eccentric eclipsing binaries. Astronomy and Astrophysics 509: A18.

Samus', N. N., Kazarovets, E. V., Durlevich, O. V., et al. 2017, Astronomy Reports, General catalogue of variable stars: Version GCVS 5.1, 61, 1, 80. doi:10.1134/S1063772917010085

Kazarovets, E. V., Samus, N. N., Durlevich, O. V., et al. 2023, Peremennye Zvezdy, The 85th Name-list of Variable Stars, 43, 9, 9. doi:10.24412/2221-0474-43-101-114

Gaia Collaboration, 2020, VizieR Online Data Catalog, I/350.

Stassun KG, Oelkers RJ, Paegert M, Torres G, Pepper J, et al. 2019. The Revised TESS Input Catalog and Candidate Target List. The Astronomical Journal 158: 138.

Bai Y, Liu J, Bai Z, Wang S, Fan D. 2019. The Astronomical Journal 158, 93.

Bellm EC, Kulkarni SR, Graham MJ, Dekany R, Smith RM, et al. 2019. PASP. 131, 018002

Lapukhin EG, Zubareva AM, Kryukova E, Khamrakulov F. 2020. Variable stars in Lacerta: area of 2°.3×2°.3, center α = 22h50m δ = 54°00·(2000.0). Part I. Peremennye Zvezdy Prilozhenie 20:2

Sokolovsky KV, Lebedev AA. 2018. VaST: A variability search toolkit. Astronomy and Computing 22: 28-4.

Jayasinghe T, Kochanek CS, Stanek KZ, Shappee BJ, Holoien TW-S, et al. 2018. The ASAS-SN catalogue of variable stars I: The Serendipitous Survey. Monthly Notices of the Royal Astronomical Society 477: 3145-63

Christy CT, Jayasinghe T, Stanek KZ, Kochanek CS, Thompson TA, et al. 2023. The ASAS-SN catalogue of variable stars X: discovery of 116 000 new variable stars using G-band photometry. Monthly Notices of the Royal Astronomical Society 519: 5271-87

Ricker GR, Winn JN, Vanderspek R, Latham DW, Bakos GÁ, et al. 2015. Transiting Exoplanet Survey Satellite (TESS). Journal of Astronomical Telescopes, Instruments, and Systems 1: 014003.

D. Handberg R, Lund MN, White TR, Hall OJ, Buzasi DL, et al. 2021. TESS Data for Asteroseismology: Photometry. The Astronomical Journal 162: 170

Claret A. 2018. A new method to compute limb-darkening coefficients for stellar atmosphere models with spherical symmetry: the space missions TESS, Kepler, CoRoT, and MOST. Astronomy and Astrophysics 618: A20

Claret A. 2000. A new non-linear limb-darkening law for LTE stellar atmosphere models. Calculations for –5.0 $\leq \log[M/H] \leq$ +1, 2000 K $\leq T_{\rm eff} \leq$ 50000 K at several surface gravities. Astronomy and Astrophysics 363: 1081-190